Hydrology and
Earth System
Sciences
Discussions

Open Access

Assessing the impact of different sources of topographic data on 1-D hydraulic modelling of floods

A. Md Ali[1,2], **D. P. Solomatine**[1,3], **and G. Di Baldassarre**[4]

[1]Department of Integrated Water System and Knowledge Management, UNESCO-IHE Institute for Water Education, Delft, the Netherlands
[2]Department of Irrigation and Drainage, Kuala Lumpur, Malaysia
[3]Water Resource Section, Delft University of Technology, Delft, the Netherlands
[4]Department of Earth Sciences, Uppsala University, Uppsala, Sweden

Correspondence to: A. Md Ali (a.ali@unesco-ihe.org)

Discussion Paper | Discussion Paper | Discussion Paper | Discussion Paper |

HESSD
11, 7375–7408, 2014

Impact of different topographic data on 1-D hydraulic modelling
A. Md Ali et al.

Title Page

Abstract   Introduction
Conclusions   References
Tables   Figures

◄◄   ►►
◄   ►

Back   Close

Full Screen / Esc

Printer-friendly Version

Interactive Discussion

Full Screen / Esc

Abstract

Topographic data, such as digital elevation models (DEMs), are essential input in flood inundation modelling. DEMs can be derived from several sources either through remote sensing techniques (space-borne or air-borne imagery) or from traditional methods (ground survey). The Advanced Spaceborne Thermal Emission and Reflection Radiometer (ASTER), the Shuttle Radar Topography Mission (SRTM), the Light Detection and Ranging (LiDAR), and topographic contour maps are some of the most commonly used sources of data for DEMs. These DEMs are characterized by different precision and accuracy. On the one hand, the spatial resolution of low-cost DEMs from satellite imagery, such as ASTER and SRTM, is rather coarse (around 30–90 m). On the other hand, LiDAR technique is able to produce a high resolution DEMs (around 1 m), but at a much higher cost. Lastly, contour mapping based on ground survey is time consuming, particularly for higher scales, and may not be possible for some remote areas. The use of these different sources of DEM obviously affects the results of flood inundation models. This paper shows and compares a number of hydraulic models developed using HEC-RAS as model code and the aforementioned sources of DEM as geometric input. The study was carried out on a reach of the Johor River, in Malaysia. The effect of the different sources of DEMs (and different resolutions) was investigated by considering the performance of the hydraulic models in simulating flood water levels as well as inundation maps. The outcomes of our study show that the use of different DEMs has serious implications to the results of hydraulic models. The outcomes also indicates the loss of model accuracy due to re-sampling the highest resolution DEM (i.e. LiDAR 1 m) to lower resolution are much less compared to the loss of model accuracy due to the use of low-cost DEM that have not only a lower resolution, but also a lower quality. Lastly, to better explore the sensitivity of the hydraulic models to different DEMs, we performed an uncertainty analysis based on the GLUE methodology.

1 Introduction

In hydraulic modelling of floods, one of the most fundamental input data is the geometric description of the floodplains and river channels often provided in the form of digital elevation models (DEM). During the past decades, there has been a significant
5 change in data collection for topographic mapping technique, from conventional ground survey to remote sensing techniques (i.e. radar wave and laser altimetry; e.g. Mark and Bates, 2000; Castellarin et al., 2009). This shift has a number of advantages in terms of processing efficiency, cost effectiveness and accuracy (Bates, 2012; Di Baldassarre and Uhlenbrook, 2012).
10 DEMs can be acquired from many sources of topographic information ranging from the high resolution and accurate, but costly, LiDAR (Light Detection and Ranging) obtained from lower altitude to low-cost, and coarse resolution, space-borne data, such as ASTER (Advanced Spaceborne Thermal Emission and Reflection Radiometer), and SRTM (Shuttle Radar Topography Mission). DEMs can also be developed from
15 traditional ground surveying (e.g. topographic contour maps) by interpolating a number of elevation points.

DEM horizontal resolution, vertical precision and accuracy varies considerably. These differences are attributed from different types of equipment and methods used in obtaining the topographic data. When used as an input to hydraulic modelling, the
20 differences in the quality of each DEM subsequently result in differences in model output performance. In addition, re-sampling processes of raster data via Geographic Information System (GIS) may also deteriorate the accuracy of the DEMs. The usefulness of diverse topographic data in supporting hydraulic modelling of floods is subject to the availability of DEMs, economic factors and geographical conditions of
25 survey area (Cobby and Mason, 1999; Casas et al., 2006; Schumann et al., 2008).

To date, a number of studies have been carried out with the aim of evaluating the impact of accuracy and precision of the topographic data on the results of hydraulic models.

Full Screen / Esc

Werner (2001) investigated the effect of varying grid element size on flood extent estimation from a 1-D model approach based on a LIDAR DEM. The study found that the flood extent estimation increased as the resolution of the DEM becomes coarser.

Horrit and Bates (2001) demonstrated the effects of spatial resolution on a raster based flood model simulation. Simulation tests were performed at resolution sizes of 10, 20, 50, 100, 250, 500, and 1000 m and the predictions were compared with satellite observations of inundated area and ground measurements of floodwave travel times. They found that the model reached a maximum performance at resolution of 100 m when calibrated against the observed inundated area. The resolution of 500 m proved to be adequate for the prediction of water levels. They also highlighted that the predicted floodwave travel times are strongly dependent on the model resolution used.

Wilson and Atkinson (2005) set up a two-dimensional (2-D) model, LISFLOOD-FP, using three different DEMs (contour dataset, synthetic-aperture radar (SAR) dataset, and differential global positioning system (DGPS)) used to predict flood inundation for 1998 flood event in the UK. The results showed that the contour datasets resulted in a substantial difference in the timing and the extent of flood inundation when compared to the DGPS dataset. Although the SAR dataset also showed differences in the timing and the extent, it was not as massive as the contour dataset. Nevertheless, the authors also highlighted a potential problem with the use of satellite remotely sensed topographic data in flood hazard assessment over small areas.

Casas et al. (2006) investigated the effects of the topographic data sources and resolution on one-dimensional (1-D) hydraulic modelling of floods. They found out that the contour-based digital terrain model (DTM) was the least accurate in the determination of the water level and inundated area of the floodplain, however the global positioning system (GPS)-based DTM lead to a more realistic estimate of the water surface elevation and of the flooded area. The LiDAR-based model produced the most acceptable results in terms of water surface elevation and inundated flooded area compared to the reference data. The authors also pointed out that the different grid sizes used in LiDAR data has no significant effect on the determination of the water

surface elevation. In addition, from an analysis of the time-cost ratio for each DEMs used, they concluded that the most cost effective technique for developing a DEM by means of an acceptable accuracy is from laser altimetry survey (LIDAR), especially for large areas.

Schumann et al. (2008) demonstrated the effects of DEMs on deriving the water stage and inundation area. Three DEMs at three different resolutions from three sources (LiDAR, contour and SRTM DEM) were used for a study area in Luxembourg. By using the HEC RAS 1-D hydraulic model to simulate the flood propagation, the result shows that, the LiDAR DEM derived water stages by displaying the lowest RMSE, followed by the contour DEM and lastly the SRTM. Considering the performance of the SRTM (it was relatively good with RMSE of 1.07 m), they suggested that the SRTM DEM is a valuable source for initial vital flood information extraction in large, homogeneous floodplains.

For the large flood prone area, the availability of DEM from public domain (e.g. ASTER, SRTM) makes it easier to conduct a study. Patro et al. (2009) selected a study area in India and demonstrated the usefulness of using SRTM DEM to derive river cross section for the use in hydraulic modelling. They found that the calibration and validation results from the hydraulic model performed quite satisfactory in simulating the river flow. Furthermore, the model performed quite well in simulating the peak flow which is important in flood modelling. The study by Tarekegn et al. (2010) carried out on a study area in Ethiopia used a DEM which was generated from ASTER image. Integration between remote sensing and GIS technique were needed to construct the floodplain terrain and channel bathymetry. From the results obtained, they concluded that the ASTER DEM is able to simulate the observed flooding pattern and inundated area extends with reasonable accuracy. Nevertheless, they also highlighted the need of advanced GIS processing knowledge when developing a digital representation of the floodplain and channel terrain.

Schumann et al. (2010) demonstrates that near real-time coarse resolution radar imagery of a particular flood event on the River Po (Italy) combined with SRTM terrain

height data leads to a water slope remarkably similar to that derived by combining the radar image with highly accurate airborne laser altimetry. Moreover, it showed that this spaceborne flood wave approximation compares well to a hydraulic model thus allowing the performance of the latter, calibrated on a previous event, to be assessed when applied to an event of different magnitude in near real time.

Paiva et al. (2011) demonstrated the use of SRTM DEM in a large-scale hydrologic model with a full one-dimensional hydrodynamic module to calculate flow propagation on a complex river network. The study was conducted on one of the major tributaries of the Amazon, the Purus River basin. They found that a model validation using discharge and water level data is capable of reproducing the main hydrological features of the Purus River basin. Furthermore, realistic floodplain inundation maps were derived from the results of the model. The authors concluded that it is possible to employ full hydrodynamic models within large-scale hydrological models even when using limited data for river geometry and floodplain characterization.

Moya Quiroga et al. (2013) used Monte Carlo simulation sampling SRTM DEM elevation, and found a considerable influence of the SRTM uncertainty on the inundation area (the HEC-RAS hydraulic model of the Timis-Bega basin in Romania was employed).

Most recently, a study by Yan et al. (2013) made a comparison between a hydraulic model based on LiDAR and SRTM DEM. Besides the DEM inaccuracy, they also introduced the uncertainty analysis by considering parameter and inflow uncertainty. The results of this study showed that the differences between the LiDAR-based model and the SRTM-based model are significant, but within the accuracy that is typically associated with large-scale flood studies.

This paper continues the presented line of research and deals with the assessment of the effect of using different DEM data source and resolution in a 1-D hydraulic modelling of floods. The novelty of this study is that both accuracy (quality) and precision (resolution) of the DEM are considered and their impact on hydraulic model results is evaluated in terms of both water surface elevation and inundation area.

Furthermore, we compare model results via independent calibration and validation and by explicitly considering parameter uncertainty.

The goal of our paper is not to validate a specific approach for producing flood inundation maps, but rather to contribute with an original approach to the existing literature exploring the impact of topographic input on hydraulic modelling of floods.

2 Study area and available data

2.1 Study area

The study area is located within the Johor River Basin in the State of Johor, Malaysia. The river basin has a total area of 2690 km^2. The test site is a 30 km reach of the Johor River. The Johor River channel has a bankfull depth between 5 and 8 m and average slope around 0.03 %. The river reach under study is characterised by a stable main channel from 50 to 250 m wide. The study area consists of agricultural land, residential and commercial areas (see Fig. 1). As reported by Department of Irrigation and Drainage, Malaysia (DID, 2009), this test site has been experiencing some major historical flood events since 1948. The most recent ones happened in December 2006 and January 2007 when more than 3000 families were evacuated.

2.2 Hydraulic modelling

In this study, hydraulic modelling of floods was performed by using the HEC-RAS modelling system. To simulate unsteady open channel flow, HEC-RAS solves the full 1-D Saint-Venant equations. The observed flow hydrograph at an hourly time step was used as upstream boundary condition, while the friction slope was used as downstream boundary condition. The next section reports the different sources of topographic data used to define the geometric input.

2.3 Digital Elevation Model

The required input data for the HEC RAS include the geometry of the floodplain and the river, which is provided by a number of cross sections. We identified several sources of DEM data for our study area (details are given below) with different spatial resolution and accuracy (Fig. 2):

1. DEMs derived from an original 1 m LiDAR dataset (obtained from DID).

2. 20 m resolution DEM generated from the vectorial 1 : 25 000 cartography map obtained from DID with a permission of the Department of Survey and Mapping, Malaysia (DSMP).

3. 30 m resolution DEM derived from the globally and freely available ASTER data retrieved from the United States Geological Survey (USGS, http://earthexplorer.usgs.gov)

4. 90 m resolution DEM derived from the globally and freely available SRTM data retrieved from a Consortium for Spatial Information (CGIAR-CSI, http://cgiar-csi.org).

To analyse the influence of spatial resolution and separate it out from the impact of different accuracy, four additional DEMs were obtained by rescaling the original LiDAR DEM (1 m resolution) to the spatial resolutions of the DEMs derived from vectorial cartography (20 m), ASTER (30 m) and SRTM (90 m). Hence, a total of eight DEMs were used (see Table 1) to explore the impact of different topographic information on the hydraulic modelling of floods.

Given that the laser/radar waves used in the remote sensing techniques are not capable of penetrating the water surface and capture the river bed elevations, all the DEMs were integrated with river cross section data derived from traditional ground survey. The ground survey of the river cross sections within the study area was systematically carried out at about 1000 m intervals. Then, the flood simulation results

across different data sets were compared to evaluate the effects of data spatial resolutions and data source differences.

3 Methodology

3.1 Evaluating the DEMs quality

At first, the vertical error of each DEM was evaluated through comparison between the topographic data and 164 Global Positioning System (GPS) ground points taken at random positions within the study area. The value of each reference elevation points were extracted from the study area using GPS survey equipment. The quality of each DEM is referred by the Root Mean Square Error (RMSE_{DEM}). The equation is as follows:

$$\text{RMSE}_{\text{DEM}} = \sqrt{\frac{\sum_{i=1}^{n}(\text{Elev}_{\text{GPS}} - \text{Elev}_{\text{DEM}})^2}{n}} \tag{1}$$

where Elev_{GPS} is the reference elevation (m) derived from GPS, Elev_{DEM} is the corresponding value derived from each DEM, and n corresponds to the total numbers of points.

3.2 Model calibration and validation

Then, data from two recent major flood events that occurred along the Johor River in 2006 and 2007 were used for independent calibration and validation of the models. The estimated peak flow of the 2006 event is approximately $375 \, \text{m}^3 \, \text{s}^{-1}$, while the one of the 2007 event is around $595 \, \text{m}^3 \, \text{s}^{-1}$. Both discharge data were measured and recorded at Rantau Panjang hydrological station. The 2006 flood data were used for the calibration exercise, while the 2007 flood data were used for model validation.

To assess the sensitivity of the different models to the model parameters, the Manning's n roughness coefficients for all the models were sampled uniformly from 0.02 to 0.08 m$^{-1/3}$ s for the river channel, and between 0.03 and 0.10 m$^{-1/3}$ s for the floodplain, by steps of 0.0025 m$^{-1/3}$ s. The performance of the hydraulic models in producing the observed water levels was assessed by means of the Mean Absolute Error (MAE):

$$\text{MAE} = \frac{1}{T} \sum_{t=1}^{T} |O_t - S_t| \tag{2}$$

where T is the number of steps in time series, O_t is the observed water level at time t, and S_t is the simulated water level at time t.

3.3 Quantifying the effect of the topographic data source on the water surface elevation and inundation area (sensitivity analysis)

The effects of DEM source and spatial resolution were further investigated by examining the sensitivity of model results in terms of maximum water surface elevation (WSE), inundation area and floodplain boundaries. For this additional analysis, the model results obtained with the most accurate and precise DEM source (LiDAR at 1 m resolution) was used as a reference. For WSE analysis, each model was compared to the reference model (Jhr L1, see Table 1) by means of the following measures:

$$\text{MAD}_{\text{WSE}} = \frac{1}{x} \sum_{x=1}^{x} |\text{WSE}_{\text{Ref}} - \text{WSE}_{\text{DEM}}| \tag{3}$$

where WSE_{Ref} denotes the WSE simulated by the reference model (Jhr L1), WSE_{DEM} the WSE estimated by the models based on DEMs of lower resolution or different source (Table 1), and x corresponds to the total number of cross sections where models results where compared.

To analyse the sensitivity to different topographic input in terms of simulated flood extent, we used the following measure of fit:

$$F(\%) = \frac{M_1 \cap M_2}{M_1 \cup M_2} \cdot 100 \tag{4}$$

where M_1 and M_2 are the simulated and observed (i.e. simulated by the reference model) inundation areas, and $\cup$ and $\cap$ are the union and intersection GIS operations respectively. F equal to 100 % indicates that the two areas are completely coincidental (Bates and De Roo, 2000).

3.4 Uncertainty estimation – GLUE analysis

In hydraulic modelling, multiple sources of uncertainty can emerge from several factors, such as model structure, topography, and friction coefficients (Aronica et al., 2002; Trigg et al., 2009; Brandimarte and Baldassarre, 2012; Dottori et al., 2013). A methodological approach to estimate the uncertainty is the generalised likelihood uncertainty estimation (GLUE) methodology (Beven and Binley, 1992), a variant of Monte Carlo simulation. Although some aspects of this methodology are criticized in several papers (e.g. Hunter et al., 2005; Mantovan and Todini, 2006; Montanari, 2005; Stedinger et al., 2008), it is still widely used in hydrological modelling because of its easiness in implementation and a common-sense approach to use only a set of the "best" models for uncertainty analysis (e.g. Hunter et al., 2005; Shrestha et al., 2009; Vázquez et al., 2009; Krueger et al., 2010; Jung and Merwade, 2012; Brandimarte and Woldeyes, 2013).

According to the GLUE framework (Beven and Binley, 1992), each simulation, i, is associated to the (generalized) likelihood weight, W_i, ranging from 0 to 1. The weight, W_i is expressed as a function of the measure fit, ε_i, of the behavioural models.

$$W_i = \frac{\varepsilon_{max} - \varepsilon_i}{\varepsilon_{max} - \varepsilon_{min}} \tag{5}$$

Title Page

Abstract | Introduction

Conclusions | References

Tables | Figures

◄◄ | ►►

◄ | ►

Back | Close

Full Screen / Esc

Printer-friendly Version

Interactive Discussion

where, ε_{max} and ε_{min} are the maximum and minimum value of MAE of behavioural models. To identify the behavioural of the models, a threshold value (rejection criteria) has been set as follows:

1. simulations associated with MAE larger than 1.0 m; and

2. Manning's n roughness coefficient of the floodplain smaller than the Manning's n roughness coefficient of the channel.

Then, the likelihood weights are the cumulative sum of 1 and the weighted 5th, 50th and 95th percentiles. The likelihood weights were calculated as follow:

$$L_i = \frac{W_i}{\sum_{i=1}^{n} W_i} \tag{6}$$

For this study, the applications of uncertainty analysis considered only the parameter uncertainty and implemented for all DEMs based model.

4   Results and discussion

4.1   Quality of DEMs compared with the reference points

Table 2 shows the calculated statistical vertical errors for each different DEM for the same study area. As anticipated, LiDAR is not only the most precise DEM because of its highest resolution, but also the most accurate. The RMSE of each LiDAR DEMs increased from 0.58 m (Jhr L1) to 1.27 m (Jhr L90) as the resolution of the DEMs reduced from 1 m (original resolution) to 90 m.

Overall, the terrain is considered well defined under the LiDAR DEMs even though the calculated errors are higher compared to the vertical accuracy reported in product specification (around 0.15 m). Figure 3 show the distribution of each DEMs compared to the GPS ground elevation.

Although LiDAR DEM gives the lowest error, it is useful to note that this type of DEM has a number of limitations as highlighted in the several papers (see Sun et al., 2003; Casas et al., 2006; Schumann et al., 2008):

1. it provides only discrete surface height samples and not continuous coverage,

2. its availability is very much limited by economic constraint,

3. its inability to capture the river bed elevations due to the fact the laser does not penetrate the water surface, and

4. its incapability to penetrate the ground surface in densely vegetated areas especially for the tropical region.

The RMSE value of the other DEMs is 4.66 m for contour maps, 7.01 m for ASTER and 6.47 m for SRTM. It's also noticeably that the RMSE of the SRTM DEM for this particular study area is within the average height accuracy found in other SRTM literature either global or at particular continent (see Table 3). Nevertheless, it is proven that this type of DEM gives an acceptable result when used in large scale flood modelling (e.g. Patro et al., 2009; Paiva et al., 2012; Yan et al., 2013).

Despite having the lowest vertical accuracies, the ASTER and contour DEMs are still widely used in the field of hydraulic flood research as they are globally available and free (e.g. Tarekegn et al., 2010; Wang et al., 2011; Gichamo et al., 2012). The differences in the vertical accuracies may partly due to the lack of information in topographical flats areas such as floodplains. However, the further use of each DEM in this study is subject to its performance in the hydraulic flood modelling during the calibration and validation stages, which are described in the following sub-section.

4.2 Model calibration and validation

Figure 4 shows the model response in terms of MAE provided by the eight models (Table 1) in simulating the 2006 flood event. In general, all models showed to be more

Title Page

Abstract | Introduction

Conclusions | References

Tables | Figures

◀ | ▶

◀ | ▶

Back | Close

Full Screen / Esc

Printer-friendly Version

Interactive Discussion

sensitivity to the changing of Manning's n roughness coefficient of main channel than the Manning's n roughness coefficient of floodplain areas. The results of the calibration showed that the best-fit models based on LiDAR DEM with different resolutions (Jhr L2, Jhr L20, Jhr L30 and Jhr L90) generally gave good performances with only slight
5 variations in the MAE value from 0.38 to 0.41 m. Nevertheless, the optimum channel and floodplain Manning's n roughness coefficient are centred on similar values at $n_{channel} = 0.0425$ to 0.0500 and $n_{floodplain} = 0.0575$ for Jhr L1, Jhr L2, Jhr L20, Jhr L30 and Jhr L90. While, the best-fit models based on topographic map and SRTM also performed well with MAE of 0.31 and 0.50 m. On the other hand, ASTER-based
10 model completely failed (exceptionally high value of MAE in Fig. 4g are due to model instabilities) and was therefore eliminated from further analysis.

The best-fit models, using the optimum Manning's n roughness coefficients (Table 4), were then used to simulate the January 2007 flood event for model validation. This was carried out for all models except ASTER based model due to its poor performance (see
15 Fig. 4g). Table 4 summarises the MAE of each model obtained during model validation. It is noted that the MAE values for all LiDAR based models (first five rows) with different resolutions remained almost the same with the difference within +0.02 m. The MAE values for the models based on topographic contour maps and SRTM DEM provides a MAE of 0.60 m.

20 The results of this first analysis suggest that the reduction in the resolution of LiDAR DEMs (from 1 to 90 m) does not significantly affect the model performance. However, the use of topographic contour maps (Jhr T20) and SRTM (Jhr S90) DEMs as geometric input to the hydraulic model produces a slight increase of model errors. For instance, Jhr L90 and Jhr S90 have the same resolution (90 m), but the different
25 accuracy results into increased (tough not remarkably) errors in model validation (from 0.39 to 0.60 m). This limited degradation of model performance (Table 4), in spite of the much lower accuracy of topographic input (Table 2) can be attributed to the fact that models are compared to water levels observed in two cross-sections. A spatially

Full Screen / Esc

Printer-friendly Version

Interactive Discussion

distributed analysis (comparing the simulated flood extent and flood water profile along the river) might show more significant differences (see Sect. 4.3).

4.3 Quantifying the effect of the topographic data source on the water surface elevation and inundation area

4.3.1 Inundation area (sensitivity analysis)

This section reports an additional analysis aiming to better explore the sensitivity of model results to different topographic data (see Sect. 3.3). Figure 5 shows the simulated flood extent maps obtained from the seven different topographic input data. The floodplain areas simulated by the five LiDAR-based models (Jhr L1, Jhr L2, Jhr L20, Jhr L30 and Jhr L90) are very similar. In contrast, the floodplain areas simulated by the models based on topographic contour maps (Jhr T20) and SRTM DEM (Jhr S90) are substantially different (see Fig. 5 and Table 5).

Table 5 shows the comparison between the different models in terms of simulating flood extent. The aforementioned measure of fit F was found to decrease for both decreasing resolution and lowering accuracy. This sensitivity analysis also shows that the results of flood inundation models are more affected by the accuracy of the DEM used as topographic input than its resolution.

4.3.2 Water surface elevation

Figure 6 compares the flood water profiles simulated by the reference model (Jhr L1) with the flood water profiles (WSE) obtained from the other six models (Jhr L2, Jhr L20, Jhr L30, Jhr L90, Jhr T20 and Jhr S90). All these flood water profiles were obtained by simulating the 2007 flood event. Despite having different resolutions, the flood water profiles simulated from all LiDAR-based models portray a similar flood water profiles to the reference model (see Fig. 6a–d). This is consistent with the findings about the

inundation area (Fig. 5). Whereas, flood water profiles simulated by the models based on topographic contour maps and SRTM DEMs (see Fig. 6e and f) are rather different.

The discrepancies between the reference model (Jhr L1) and the other models visualized in Fig. 6 are quantified in terms of Mean Absolute Difference (MAD). This shows that the re-sampled LiDAR data (Jhr L2, Jhr L20, Jhr L30 and Jhr L90) have all a low MAD: between 0.05 to 0.08 m. Higher discrepancies are found with the models based on SRTM DEM (0.76 m) and contour maps (1.12 m). The great differences obtained using the topographic contour maps may be partly due to the way that the DEM height is sampled. For instance, contour DEM in this study were based on topographic contours at 20 m intervals and required interpolation technique to generate a DEM. Table 6 shows the summary of MAD in terms of water surface elevation simulated by the models.

4.3.3 Uncertainty in flood profiles obtained from different DEMs model by considering parameter uncertainty

To better interpret the differences that have emerged in comparing the results of models based on different topographic data, we carried out a set of numerical experiments to explore the uncertainty in model parameters. As mentioned, we varied the Manning's n roughness coefficient between 0.02 and 0.08 $m^{-1/3}$ s, for the river channel, and from 0.03 to 0.10 $m^{-1/3}$ s, for the floodplain, with steps 0.0025 $m^{-1/3}$ s. Then, a number of simulations are reject as described in Sect. 3.4. Figure 7 shows the uncertainty bounds for the different models. The width of these uncertainty bounds was found to be between 1.5 and 1.6 m for all models (only parameter uncertainty is considered here). Nevertheless, the model based on contour maps lead to significant differences from the LiDAR based model, even when the uncertainty induced by model parameters is expletively accounted for (see Fig. 7e).

5 Conclusions

This study assessed how different DEMs (derived by various sources of topographic information or diverse resolutions) affect the output of hydraulic modelling. A reach of the Johor River, Malaysia, was used as the test site. The sources of DEMs were LiDAR at 1 m resolution, topographic contour maps at 20 m resolution, ASTER data at 30 m resolution, and SRTM data at 90 m resolution. The LiDAR DEM was also re-sampled from its original resolution dataset to 2, 20, 30, and 90 m cell size. Different models were built by using them as geometric input data.

The performance of the five LiDAR-based models (characterised by different resolutions ranging from 1 to 90 m; see Table 4) did not show significant differences. Neither in the exercise of independent calibration and validation based on water level observations in an internal cross section, nor in the sensitivity analysis of simulated flood profiles and inundation areas. Another striking result of our study is that the model based on ASTER data completely failed because of major inaccuracies of the DEM.

In contrast, the models based on SRTM data and topographic contour maps did relatively well in the validation exercise as they provided a mean absolute error of 0.6 m, which is only slightly higher the ones obtained with LiDAR-based models (all around 0.4 m). However, this outcome could be attributed to the fact that validation could only be performed by using the water level observed in a two internal cross-sections. As a matter of fact, higher discrepancies emerged when LiDAR-based models are compared to the models based on SRTM data or topographic contour maps in terms of inundation areas or flood water profiles. These differences were found to be relevant even when parameter uncertainty is accounted for.

The study also showed that, to support flood inundation models, the quality and accuracy of the DEM is more relevant than the resolution and precision of the DEM. For instance, the model based on the 90 m DEM obtained by re-sampling the LiDAR data performed better than model based on the 90 m DEM obtained from SRTM data. These outcomes are unavoidably associated to the specific test site, but the

methodology proposed here can allow a comprehensive assessment of the impact of diverse topographic data on hydraulic modelling of floods for different rivers around the world.

References

Aronica, G., Bates, P. D., and Horritt, M. S.: Assessing the uncertainty in distributed model predictions using observed binary pattern information within GLUE, Hydrol. Process., 16, 2001–2016, doi:10.1002/hyp.398, 2002.

Bates, P. D.: Integrating remote sensing data with flood inundation models: how far have we got?, Hydrol. Process., 26, 2515–2521, doi:10.1002/hyp.9374, 2012.

Bates, P. D. and De Roo, A. P. J.: A simple raster-based model for floodplain inundation, J. Hydrol., 236, 54–77, 2000.

Berry, P. A. M., Garlick, J. D., and Smith, R. G.: Near-global validation of the SRTM DEM using satellite radar altimetry, Remote Sens. Environ., 106, 17–27, doi:10.1016/j.rse.2006.07.011, 2007.

Beven, K. and Binley, A.: The future of distributed models – model calibration and uncertainty prediction, Hydrol. Process., 6, 279–298, doi:10.1002/hyp.3360060305, 1992.

Brandimarte, L. and Di Baldassarre, G.: Uncertainty in design flood profiles derived by hydraulic modelling, Hydrol. Res., 43, 753–761, doi:10.2166/nh.2011.086, 2012.

Brandimarte, L. and Woldeyes, M. K.: Uncertainty in the estimation of backwater effects at bridge crossings, Hydrol. Process., 27, 1292–1300, doi:10.1002/hyp.9350, 2013.

Casas, A., Benito, G., Thorndycraft, V. R., and Rico, M.: The topographic data source of digital terrain models as a key element in the accuracy of hydraulic flood modelling, Earth Surf. Proc. Land., 31, 444–456, doi:10.1002/esp.1278, 2006.

Castellarin, A., Di Baldassarre, G., Bates, P. D., and Brath, A.: Optimal cross-section spacing in Preissmann scheme 1D hydrodynamic models, J. Hydraul. Eng.-ASCE, 135, 96–105, doi:10.1061/(ASCE)0733-9429(2009)135:2(96), 2009.

Cobby, D. M. and Mason, D. C.: Image processing of airborne scanning laser altimetry for improved river flood modelling, ISPRS J. Photogramm., 56, 121–138, 1999.

Di Baldassarre, G. and Uhlenbrook, S.: Is the current flood of data enough? A treatise on research needs for the improvement of flood modelling, Hydrol. Process., 26, 153–158, doi:10.1002/hyp.8226, 2012.

Dottori, F., Di Baldassarre, G., and Todini, E.: Detailed data is welcome, but with a pinch of salt: accuracy, precision, and uncertainty in flood inundation modelling, Water Resour. Res., 49, 6079–6085, doi:10.1002/wrcr.20406, 2013.

Farr, T. G., Rosen, P. A., Caro, E., Crippen, R., Duren, R., Hensley, S., Kobrick, M., Paller, M., Rodriguez, E., Roth, L., Seal, D., Shaffer, S., Shimada, J., Umland, J., Werner, M., Oskin, M., Burbank, D., and Alsdorf, D.: The shuttle radar topography mission, Rev. Geophys., 45, RG2004, doi:10.1029/2005RG000183, 2007.

Gichamoa, T. Z., Popescu, I., Jonoski, A., and Solomatine, D.: River cross-section extraction from the ASTER global DEM for flood modelling, Environ. Modell. Softw., 31, 37–46, doi:10.1016/j.envsoft.2011.12.003, 2012.

Horrit, M. S. and Bates, P. D.: Effects of spatial resolution on a raster based model of flood flow, J. Hydrol., 253, 239–249, 2001.

Hunter, N. M., Bates, P. D., Horritt, M. S., De Roo, A. P. J., and Werner, M. G. F.: Utility of different data types for calibrating flood inundation models within a GLUE framework, Hydrol. Earth Syst. Sci., 9, 412–430, doi:10.5194/hess-9-412-2005, 2005.

Jung, Y. and Merwade, V.: Uncertainty quantification in flood inundation mapping using generalized likelihood uncertainty estimate and sensitivity analysis, J. Hydrol. Eng., 17, 507–520, 2012.

Krueger, T., Freer, J., Quinton, J. N., Macleod, C. J. A., Bilotta, G. S., Brazier, R. E., Butler, P., and Haygarth, P. M.: Ensemble evaluation of hydrological model hypotheses, Water Resour. Res., 46, W07516, doi:10.1029/2009WR007845, 2010.

Mantovan, P. and Todini, E.: Hydrological forecasting uncertainty assessment: incoherence of the GLUE methodology, J. Hydrol., 330, 368–381, doi:10.1016/j.jhydrol.2006.04.046, 2006.

Marks, K. and Bates, P. D.: Integration of high resolution topographic data with floodplain flow models, Hydrol. Process., 14, 2109–2122, 2000.

Montanari, A.: Large sample behaviors of the generalized likelihood uncertainty estimation (GLUE) in assessing the uncertainty of rainfall–runoff simulations, Water Resour. Res., 41, W08406, doi:10.1029/2004WR003826, 2005.

Title Page

Abstract | Introduction

Conclusions | References

Tables | Figures

⏮ | ⏭

◀ | ▶

Back | Close

Full Screen / Esc

Printer-friendly Version

Interactive Discussion

Moya Quiroga, V., Popescu, I., Solomatine, D. P., and Bociort, L.: Cloud and cluster computing in uncertainty analysis of integrated flood models, J. Hydroinform., 15, 55–69, doi:10.2166/hydro.2012.017, 2013.

Paiva, R. C. D., Collischonn, E., and Tucci, C. E. M.: Large scale hydrologic and hydrodynamic modeling using limited data and a GIS based approach, J. Hydrol., 406, 170–181, doi:10.1016/j.jhydrol.2011.06.007, 2011.

Patro, S., Chatterjee, C., Singh, R., and Raghuwanshi, N. S.: Hydrodynamic modelling of a large flood-prone system in India with limited data, Hydrol. Process., 23, 2774–2791, doi:10.1002/hyp.7375, 2009.

Rabus, B., Eineder, M., Roth, A., and Bamler, R.: The shuttle radar topography mission – a new class of digital elevation models acquired by spaceborne radar, ISPRS J. Photogramm., 57, 241–262, doi:10.1016/S0924-2716(02)00124-7, 2003.

Rodríguez, E., Morris, C. S., Belz, J. E., Chapin, E. C., Martin, J. M., Daffer, W., and Hensley, S.: An assessment of the SRTM topographic products, Technical Report JPL D-31639, Jet Propulsion Laboratory, Pasadena, California, 143 pp., available at: http://www2.jpl.nasa.gov/srtm/srtmBibliography.html (last access: 16 December 2013), 2005.

Schumann, G., Matgen, P., Cutler, M. E. J., Black, A., Hoffmann, L., and Pfister, L.: Comparison of remotely sensed water stages from LiDAR, topographic contours and SRTM, ISPRS J. Photogramm., 63, 283–296, 2008.

Schumann, G., Di Baldassarre, G., Alsdorf, D., and Bates, P. D.: Near real-time flood wave approximation on large rivers from space: application to the River Po, Northern Italy, Water Resour. Res., 46, W05601, doi:10.1029/2008WR007672, 2010.

Shrestha, D. L., Kayastha, N., and Solomatine, D. P.: A novel approach to parameter uncertainty analysis of hydrological models using neural networks, Hydrol. Earth Syst. Sci., 13, 1235–1248, doi:10.5194/hess-13-1235-2009, 2009.

Stedinger, J. R., Vogel, R. M., Lee, S. U., and Batchelder, R.: Appraisal of the generalized likelihood uncertainty estimation (GLUE) method, Water Resour. Res., 44, W00B06, doi:10.1029/2008WR006822, 2008.

Sun, G., Ranson, K. J., Kharuk, V. I., and Kovacs, K.: Validation of surface height from shuttle radar topography mission using shuttle laser altimetry, Remote Sens. Environ., 88, 401–411, doi:10.1016/j.rse.2003.09.001, 2003.

Title Page

Abstract | Introduction

Conclusions | References

Tables | Figures

|◄ | ►|

◄ | ►

Back | Close

Full Screen / Esc

Printer-friendly Version

Interactive Discussion

Tarekegn, T. H., Haile, A. T., Rientjes, T., Reggiani, P., and Alkema, D.: Assessment of an ASTER generated DEM for 2D flood modelling, Int. J. Appl. Earth Obs., 12, 457–465, doi:10.1016/j.jag.2010.05.007, 2010.

Trigg, M. A., Wilson, M. D., Bates, P. D., Horritt, M. S., Alsdorf, D. E., Forsberg, B. R., and Vega, M. C.: Amazon flood wave hydraulics, J. Hydrol., 374, 92–105, 2009.

Vázquez, R. F., Beven, K., and Feyen, J.: GLUE based assessment on the overall predictions of a MIKE SHE application, Water Resour. Res., 23, 1325–1349, doi:10.1007/s11269-008-9329-6, 2009.

Wang, W., Yang, X., and Yao, T.: Evaluation of ASTER GDEM and SRTM and their suitability in hydraulic modelling of a glacial lake outburst flood in southeast Tibet, Hydrol. Process., 26, 213–225, doi:10.1002/hyp.8127, 2011.

Werner, M. G. F.: Impact of grid size in GIS based flood extent mapping using a 1D flow model, Phys. Chem. Earth B, 26, 517–522, 2001.

Wilson, M. D. and Atkinson, P. M.: The use of elevation data in flood inundation modelling: a comparison of ERS interferometric SAR and combined contour and differential GPS data, International Journal of River Basin Management, 3, 3–20, doi:10.1080/15715124.2005.9635241, 2005.

Yan, K., Di Baldassarre, G., and Solomatine, D. P.: Exploring the potential of SRTM topographic data for flood inundation modelling under uncertainty, J. Hydroinform., 15, 849–861, doi:10.2166/hydro.2013.137, 2013.

Table 1. Information about the eight digital elevation models used as topographical input.

Model name	DEM type	Resolution (m)
Jhr L1	LiDAR	1 m
Jhr L2	(re-scaled from LiDAR)	2 m
Jhr L20	(re-scaled from LiDAR)	20 m
Jhr L30	(re-scaled from LiDAR)	30 m
Jhr L90	(re-scaled from LiDAR)	90 m
Jhr T20	Contours maps	20 m
Jhr A30	ASTER	30 m
Jhr S90	SRTM	90 m

Table 2. Statistics of errors (m) of each DEMs with respect to the GPS control points.

Model name	Min. error (m)	Max. error (m)	RMSE (m)
Jhr L1	−0.59	1.00	0.58
Jhr L2	−0.64	1.38	0.58
Jhr L20	−0.83	1.83	0.68
Jhr L30	−0.93	3.98	0.79
Jhr L90	−5.46	3.73	1.27
Jhr T20	−15.38	10.55	4.66
Jhr A30	−33.37	7.58	7.01
Jhr S90	−3.59	4.32	6.47

Table 3. Reported vertical accuracies of SRTM data.

Reference	Average height accuracy (m)	Continent
Rabus et al. (2003)	6.00	European
Sun et al. (2003)	11.20	European
SRTM mission specification (Rodriguez et al., 2005)	16.00	Global
Berry et al. (2007)	2.54	Eurasia
	3.60	Global
Farr et al. (2007)	6.20	Eurasia
Wang et al. (2011)	13.80	Eurasia

Table 4. Model validation results.

Model name	Calibrated Manning's n roughness coefficient		MAE (m) (validation)
	channel	floodplain	
Jhr L1	0.0500	0.0575	0.40
Jhr L2	0.0450	0.0575	0.38
Jhr L20	0.0425	0.0575	0.37
Jhr L30	0.0450	0.0575	0.38
Jhr L90	0.0450	0.0550	0.39
Jhr T20	0.0500	0.0750	0.60
Jhr S90	0.0375	0.0500	0.60

Table 5. Effects of DEMs (source and resolution) on HEC-RAS simulations.

Model name	Inundation area (km^2)	Area difference (%)	F (%)	F^* (%)
Jhr L1	25.86	–	–	–
Jhr L2	25.78	−0.3	96.6	–
Jhr L20	25.96	0.4	92.9	–
Jhr L30	26.18	1.2	92.2	–
Jhr L90	25.84	−0.1	89.4	–
Jhr T20	29.23	13.0	73.7	74.2
Jhr S90	16.58	−35.9	48.9	49.6

* Overlap-fit percentage F (%) of the floodplain inundated area with those from LiDAR DEMs of the same resolutions (Jhr L20, Jhr L90).

Table 6. Summary of Mean Absolute Difference (MAD) in terms of water surface elevation simulated by the models.

Model name	MAD_{WSE} (m)
Jhr L1	–
Jhr L2	0.06
Jhr L20	0.05
Jhr L30	0.05
Jhr L90	0.08
Jhr T20	1.12
Jhr S90	0.76

Full Screen / Esc

Printer-friendly Version

Interactive Discussion
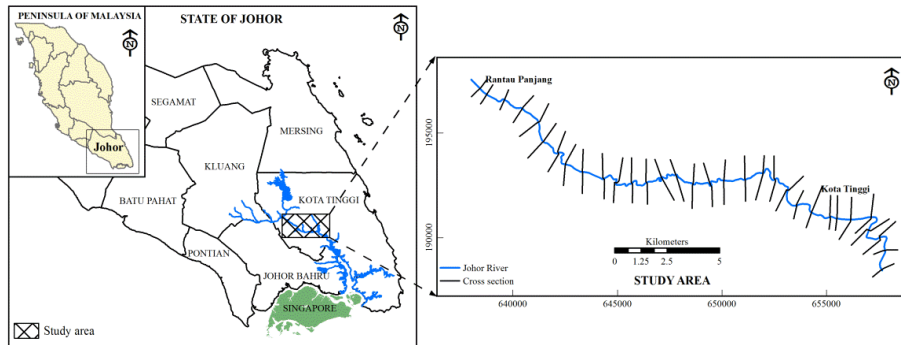
Figure 1. Layout map of study area: Johor River, Malaysia.

Figure 2. Original DEMs used in this study, based on: **(a)** LiDAR data; **(b)** Contour map; **(c)** ASTER data; and **(d)** SRTM data.
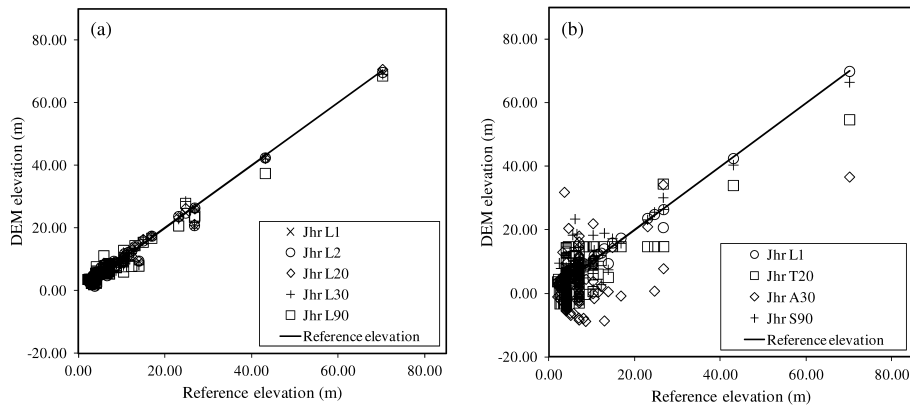
Figure 3. Comparison between GPS point elevations and elevations derived by the different DEMs: **(a)** LiDAR DEM at different resolution; and **(b)** different sources of DEMs.

Full Screen / Esc

Printer-friendly Version

Interactive Discussion
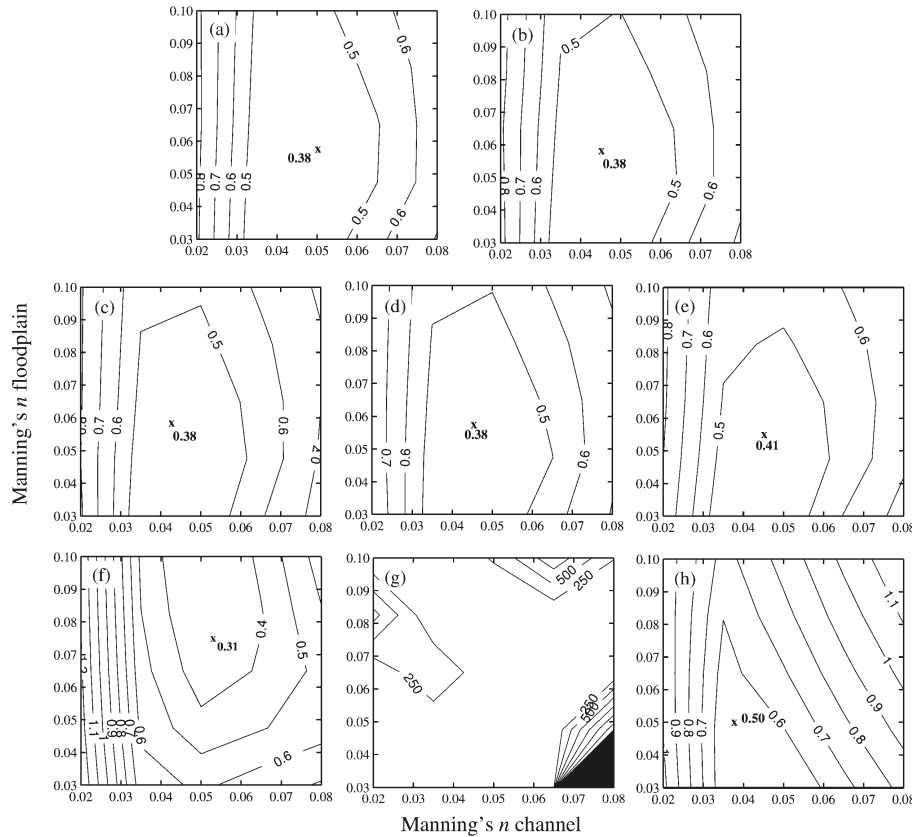
Figure 4. Contour map of MAE across the parameter space for eight different models (see Table 1): **(a)** Jhr L1, **(b)** Jhr L2, **(c)** Jhr L20, **(d)** Jhr L30, **(e)** Jhr L90, **(f)** Jhr T20, **(g)** Jhr A30, and **(h)** Jhr S90.
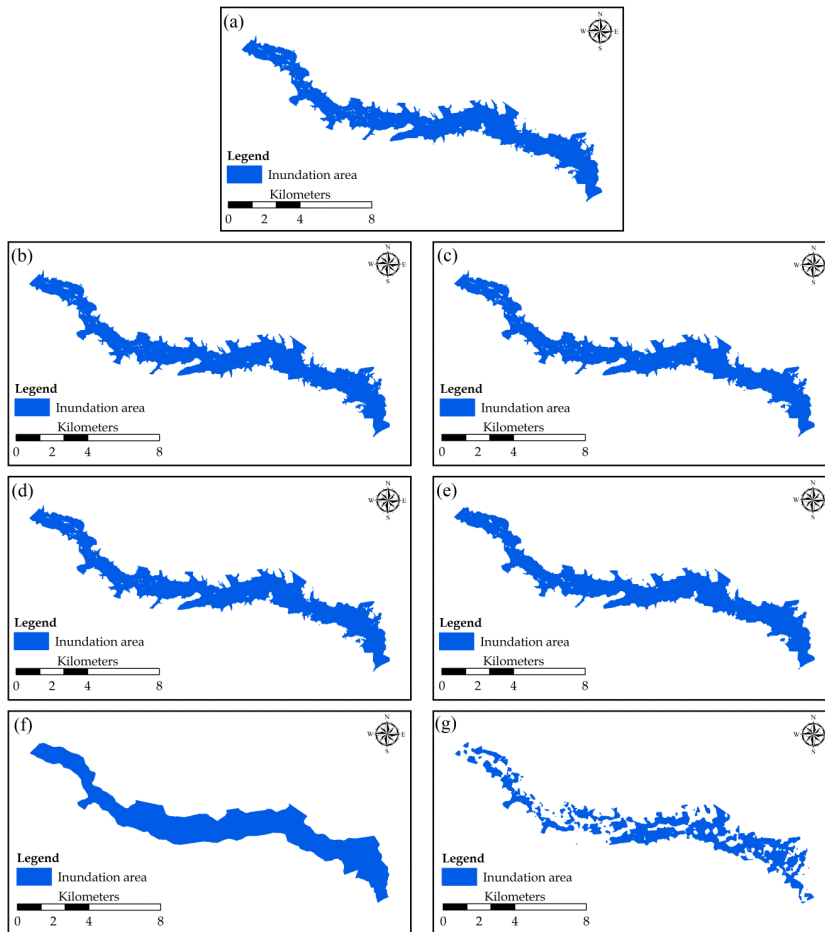
Figure 5. Effect of DEMs on Johor River. Inundation map resulting from **(a)** Jhr L1; **(b)** Jhr L2; **(c)** Jhr L20; **(d)** Jhr L30; **(e)** Jhr L90; **(f)** Jhr T20, and **(g)** Jhr S90.
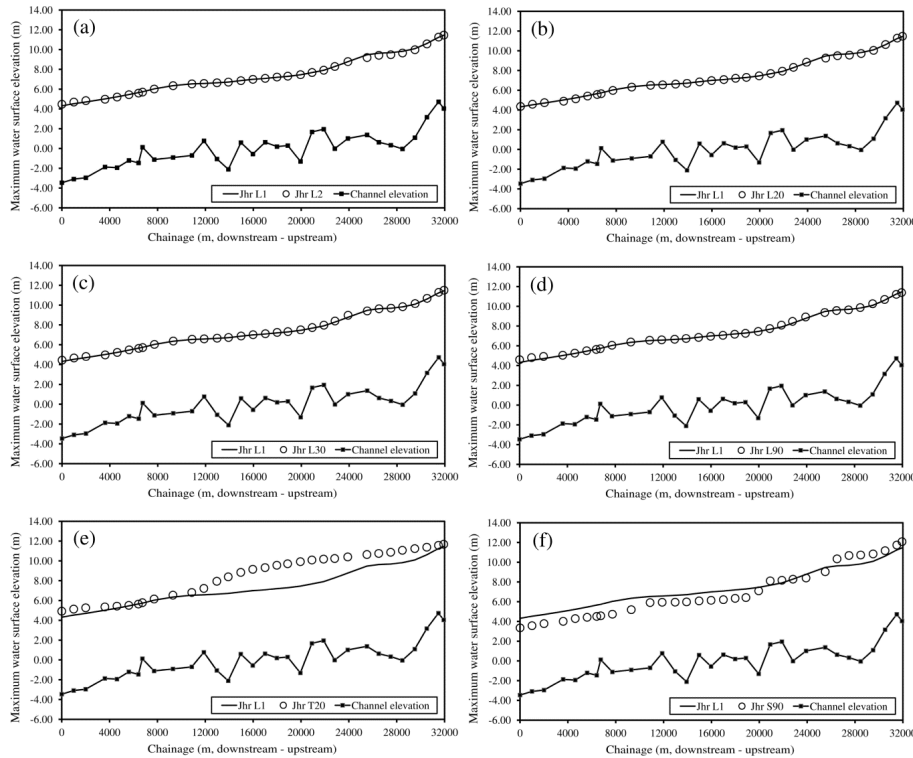
Figure 6. Maximum water surface elevation along the Johor River for the six hydraulic models compared to that simulated by the reference model.
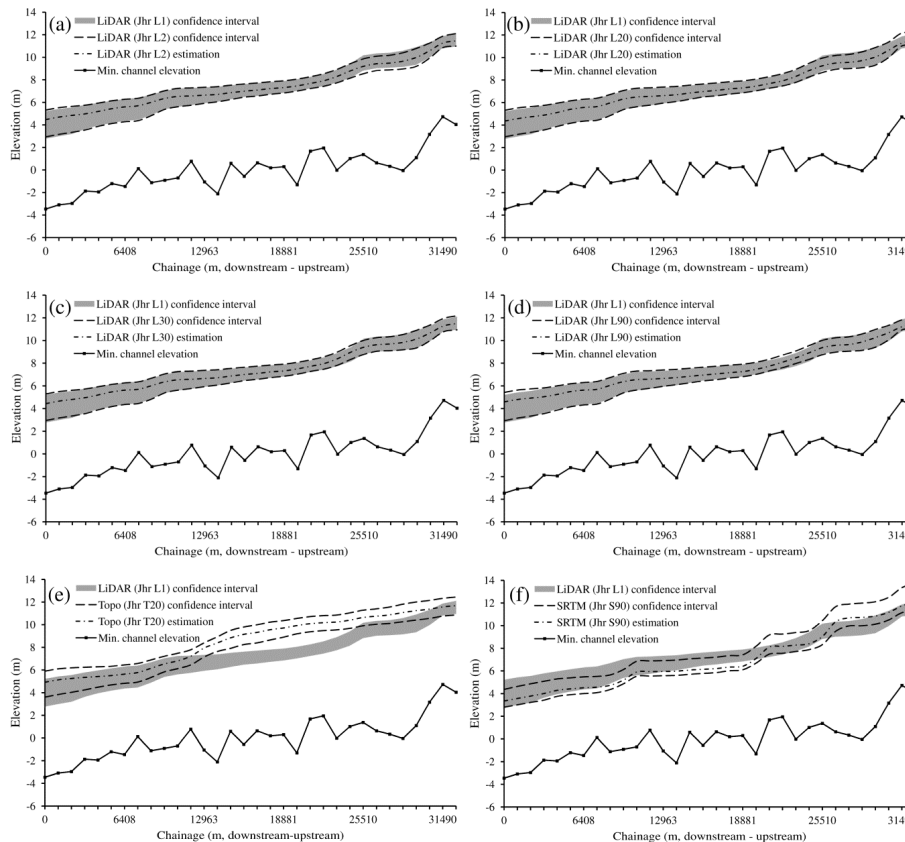
Figure 7. Comparison of uncertainty bounds (5th, 50th and 95th percentiles by considering parameter uncertainty only) between the reference model and the other models. The reference model uncertainty bound are shown in gray areas, while the uncertainty bound of the other six models are shown in dashed line.